



Kinetic, equilibrium, and thermodynamic study on atrazine adsorption in organophilic clay

Fernando Manzotti de Souza^{a,*}, Angélica Machi Lazarin^b, Melissa Gurgel Adeodato Vieira^c, Onélia Aparecida Andreo dos Santos^a

^aDepartment of Chemical Engineering, State University of Maringá, Av. Colombo, nº. 5790, 87.020.900 Maringá, Paraná, Brazil, Tel. +55 44 997622074, email: fernandomanzotti@outlook.com (F.M. de Souza)

^bDepartment of Chemistry, State University of Maringá, Av. Colombo, no. 5790, 87020-900, Maringá, Paraná, Brazil

^cSchool of Chemical Engineering, University of Campinas, Av. Albert Einstein, no. 500, 13083-852, Campinas, São Paulo, Brazil

Received 8 February 2018; Accepted 7 July 2018

ABSTRACT

The organophilic clay used as adsorbent in this work was obtained from the modification of the commercial Fluidigel clay with the hexadecyltrimethylammonium bromide salt by the chemical synthesis process. The commercial and modified adsorbent materials were characterized by N₂ physics, scanning electron microscopy (SEM), thermal analysis (TGA/DTA), X-ray diffraction (XRD), energy dispersive system (EDX), and Fourier-transform infrared spectroscopy (FTIR), aiming to determine possible structural, morphological, structural, and chemical changes promoted by the organophilization stage. The kinetic, equilibrium, and thermodynamic aspects of the atrazine adsorption process were investigated by using the synthesized material. In the optimization of the parameters, it was verified that the pH did not influence significantly the adsorption. The kinetic model that best represented the data was that proposed by Elovich and through the equilibrium isotherms and thermodynamic analysis, it was verified that the material has heterogeneous active sites and that the process is favorable, reaching maximum values of adsorption capacity of up to 3.492 mg g⁻¹, thus highlighting the good performance of the material when compared with other alternative adsorbents in the removal of atrazine in contaminated water.

Keywords: Organophilic clay; Characterization; Adsorption; Atrazine

1. Introduction

The contamination of aquatic matrices is a widespread problem. The quality of the water in the world has been suffering due to the significant increase in the presence of micropollutants of anthropic origin in the water matrices, among them stand out substances such as human and veterinary pharmaceuticals, personal care, surfactants, pesticides, dyestuffs from the food and textile industries, disinfectants, and other chemical additives that are used in large quantities every year all over the world [1–6].

Of the aforementioned categories, pesticides have a prominent character as a contaminant. In the United States, for example, the national water quality assessment program Geological Survey mentions that 95% of surface water and 50% of groundwater contain at least one pesticide in its composition. In the European Union, 700 synthetic substances were detected in water for human consumption, of which 300 were pesticides [7,8].

Since 2008, Brazil has been the largest consumer of agrochemicals in the world [9]. Its major applications are divided between soya, maize, sugarcane, and cotton crops. In the 2011 harvest, about 71 million hectares of temporary and permanent crops were planted, equivalent to a value of 853 million liters of pesticides used in these plantations, mainly herbicides, fungicides, and insecticides, representing an average

* Corresponding author.

use of 12 L ha⁻¹ and an average environmental/occupational/food exposure of 4.5 L of pesticides per inhabitant [10].

In Brazil from 2009 to 2012, the most consumed agrochemicals were glyphosate, 2,4-d, atrazine, carbendazim, and diuron [11]. The presence of atrazine, simazine, imidacloprid, chlorpyrifos, and clomazone in surface water from three basins of Rio Grande do Sul in areas of tobacco culture was evaluated. Glyphosate was found in several points of the Pirapó River in the city of Maringá, state of Paraná – near soybean plantations and there was also evidence of atrazine and endosulfan in 16 samples of water in streams of Campo Verde, state of Mato Grosso [12–14].

With between 70,000 and 90,000 tonnes being applied per year, atrazine (1-chloro-3-ethylamino-5-isopropylamino-2,4,6-triazine) is one of the main herbicides in the triazine class, widely used against pests, especially in sugarcane, soybean, maize, and sorghum [15]. This herbicide is extremely toxic; it is a carcinogenic agent and an endocrine disruptor. Exposure to it may increase the appearance of cancer, cause neuroendocrine effects in vertebrates that lead to irregular ovary functioning, and cause various genomic changes [16–18]. Maximum concentration limits in water for human consumption are determined because of its high toxicity. In Europe, for instance, this limit is 0.1 µg L⁻¹; in Brazil, 2 µg L⁻¹; and in the United States, it is as high as 3 µg L⁻¹ [19,20].

Conventional water treatment techniques are used for the removal of atrazine and other pesticides from water for human consumption. Among those, the most common are coagulation, flocculation, clarification, and chlorination, but unfortunately, these are incapable of eliminating these organic compounds effectively [8]. Recent studies have looked at evaluating the effectiveness of advanced treatment techniques, such as chemical oxidation, biodegradation, and photodegradation, aiming at eliminating pesticides as well as other natural organic pollutants. Despite these qualities, several of these procedures have high costs and operational complexity, compromising their applicability in water treatment plants.

Due to its high-efficiency, low-cost operation with no relevant byproducts, since a great part of adsorbents can be regenerated; adsorption has become a frequently sought alternative for removing organic and inorganic pollutants. It is also easily implementable in water treatment plants after the conventional treatment methods. Nevertheless, the cost of the adsorbent may sometimes make the procedure unviable, so studying alternative efficient adsorbents is an important step for the optimization and enabling of this technique [2,21].

Clays are materials with a high capacity for cation exchange and low cost because of its high environmental abundance [22]. In their natural form, clays are hydrophilic, thus not showing efficient organic compound adsorption. However, when exposed to chemical treatments, such as with cationic surfactants, their surface is modified and they begin to show hydrophobic and organophilic characteristics, acquiring high affinity for organic molecules [23].

Promising results can be found in scientific literature regarding clay usage in water treatment, with clays having shown excellent performance in the removal of petrochemical organic compounds, such as toluene, and also in the treatment of water polluted with Paraquat herbicide [24,25].

Therefore, this paper aimed at synthesizing and characterizing organophilic clay, evaluating its textural, morphological, structural, and chemical characteristics, and in regards to the resulting adsorbent, investigating its kinetic, equilibrium, and thermodynamic aspects in the adsorption of atrazine.

2. Material and methods

2.1. Organophilic clays preparation

The organophilic clay was prepared from sodium bentonite clay, coming from the city of Boa Vista, state of Paraíba, Brazil, commercialized as Fluidgel and processed by Dolomil Ltda Company. The chemical synthesis stage was carried out according to the methodology proposed by Barbosa et al. [26]. A beaker containing 1,600 mL of deionized water was put on a heater with a controlled temperature between 80°C ± 5°C. Afterward, 32 g of clay and 20 g of quaternary ammonium salt hexadecyltrimethylammonium bromide – HDTMA (Merck) were slowly added with continuous mechanical agitation and were kept in this way for 20 min. The HDTMA mass was calculated from the cation-exchange capacity of the commercial clay, which amounts to 171.74 meq/100 g of clay. After this period, the recipient was closed and kept in room temperature for 24 h. The synthesized adsorbent drying was made in an oven between 60°C ± 5°C for 48 h, soon after, it was ground in a mortar and sifted in order to obtain medium-sized diameter particles of 0.855 mm.

2.2. Commercial and organophilic clay characterization

The clays were characterized by X-ray diffraction (XRD), N₂ physisorption, Fourier-transform infrared spectroscopy (FTIR), scanning electron microscopy (SEM), thermal gravimetric analysis (TGA), and differential thermal analysis (DTA).

The X-ray diffractometers were obtained in a Bruker Diffractometer, D8 advance series within the 2θ = 2–30 range, with copper Ka radiation, 40 kV tension, 30 mA current, and 2° min⁻¹ scanning speed [26].

The identification of functional groups was made in a PerkinElmer Spectrophotometer, spectrum 100 series through the self-supported wafer method in KBr with a spectral span of 4,000–400 cm⁻¹ [27].

The textural characteristics of the adsorbents were found through isotherms of adsorption and desorption of nitrogen on the surface of 77 K (–196°C) clays, being held in the Quantachrome measurer NOVA 1,000 series with the activation of the material being done at 373 K (100°C). The specific area of each sample was calculated by using the BET method, proposed Brunauer, Emmett, and Teller [28], and the average volume of the pores was found based on the BJH calculations [29].

The SEM images were acquired in the FEI Company equipment, Quanta-250 series with an acceleration voltage of 20 kV. The samples were prepared in an aluminum structure above a carbon tape with a thin layer of gold coating through a metalizer.

The TGA was collected in a Shimadzu thermogravimetric analyzer, TGA-50 series with a programmed temperature increase, from room temperature to 1,000°C with nitrogen flow of 50 mL min⁻¹ and heating speed of 10°C min⁻¹ [30].

2.3. Analytical determination of atrazine concentration

Atrazine was analyzed by using an UV-vis Shimadzu spectrophotometer UV-1,800 series. The preparation of the calibration curve was made from a stock standard solution from 250 mg L⁻¹ (Sigma-Aldrich, Brazil) in methanol pattern HPLC (JTBaker, Brazil) with a variation from 1 to 10 mg L⁻¹. Reading was carried out in a 222 nm absorbance, value referring to the peak of maximum absorption [31].

3. Adsorption experiments

3.1. Adsorbent dosage and pH effect

The effect of pH was monitored with a fixed amount of organophilic clay of 4 g L⁻¹ in a 125 mL Erlenmeyer flask containing 25 mL of atrazine solution with pH in the range of 2–12 adjusted with NaOH solution (0.1 M) and HCl (0.1 M), both analytical standards (Synth), fixed herbicide concentration at 5 mg L⁻¹, invariable temperature (25.0°C ± 0.5°C) and continuous movement using a Dubnoff type reciprocating stirrer in a 24 h period. After the samples were collected, filtered on 0.22 µm cellulose nitrate membranes and then analyzed. As a response variable the percentage removal [Eq. (1)] was considered as follows:

$$\% \text{Removal} = \frac{(C_0 - C_e)}{C_0} \times 100 \quad (1)$$

where C_0 its initial concentration of atrazine (mg L⁻¹) and C_e its equilibrium concentration (mg L⁻¹).

The dosage of adsorbent as well as the pH can exert influence during the process of micropollutants removal from contaminated water. The adsorbent concentration (4, 8, 12, 16, and 20 g L⁻¹) was investigated by using the same experimental conditions described earlier. The pH was kept constant (7 ± 1).

3.2. Kinetic assays

The kinetic experiments were conducted in a 125 mL Erlenmeyer flask in discontinuous ways (batch type), invariable ambient temperature (25.0°C ± 0.5°C), neutral pH (7 ± 1), adsorbent concentration of 20 g L⁻¹, and fixed atrazine solution (5, 10, and 15 mg L⁻¹). The time intervals established for aliquot withdrawal were 1, 5, 10, 20, 30, 40, 60, 90, 120, 150, 180, and 240 min.

The adsorption capability q_t (mg adsorbate g⁻¹ de adsorbent) at each moment was found by Eq. (2) as follows:

$$q_t = \frac{(C_0 - C(t)) \times V}{m} \quad (2)$$

where C_0 is the initial concentration of atrazine used in the test (mg L⁻¹), $C(t)$ is the equilibrium concentration at each determined moment t (mg L⁻¹), V represents the volume of solution (mL), and m is the mass of adsorbent used (g).

The pseudo-first-order [32], pseudo-second-order [33], and Elovich [34] mathematical models were fitted to the kinetic data in order to understand the types of mechanisms

involved in the adsorption process. These models are shown in Eqs. (3), (4), and (5) as follows:

$$q_t = q_e \left(1 - e^{(-k_1 t)}\right) \quad (3)$$

$$q_t = \frac{k_2 q_e^2 t}{1 + k_2 q_e t} \quad (4)$$

$$q_t = \frac{1}{b} \times \ln(1 + abt) \quad (5)$$

where q_e and q_t are the adsorption capabilities of atrazine (mg g⁻¹) at equilibrium and at moment t , k_1 is the pseudo-first-order rate of constant speed (min⁻¹), k_2 is the pseudo-second-rate of constant speed (g mg⁻¹ min⁻¹), a is the initial adsorption rate (mg g⁻¹ min⁻¹), and b represents the desorption constant (g mg⁻¹).

The intraparticle diffusion [35] [Eq. (6)] and Boyd [36] [Eq. (7)] models were applied to evaluate the process steps that limit the adsorption as follows:

$$q_t = k_{\text{dif}} t^{1/2} + C \quad (6)$$

$$F = 1 - (6\pi^2)^{-1} \times e^{-B_i} \quad (7)$$

$$F = \frac{q_t}{q_e} \quad (8)$$

where k_i is the diffusion rate constant between particles (mg g⁻¹ min^{-1/2}), C represents the boundary layer thickness (mg g⁻¹), and B_i is the Boyd constant.

The value of B_i is determined from Eqs. (9) to (10) as a function of the F value [37]:

$$F > 0.85 \quad B_i = -0.4977 - \ln(1 - F) \quad (9)$$

$$F < 0.85 \quad B_i = \left(\sqrt{\pi} - \sqrt{\pi - \frac{\pi^2 F}{3}} \right)^2 \quad (10)$$

Using the coefficient obtained by the graph of $B_i \times t$, we can calculate the effective diffusivity coefficient D_i (cm² min⁻¹) described by Eq. (11) as follows:

$$B_i = \frac{\pi^2 D_i}{r^2} \quad (11)$$

where r is the radius of the adsorbent particle (cm).

3.3. Equilibrium adsorption assays

The equilibrium isotherms were carried out at different temperatures (25°C, 35°C, and 45°C) and initial concentrations (2–60 mg L⁻¹), pH 7 ± 1, and fixed adsorbent concentration (20 g L⁻¹) in 125 mL Erlenmeyer flask. The equilibrium adsorption capacity was determined by Eq. (12) as follows:

$$q_e = \frac{(C_0 - C_e) \times V}{m} \quad (12)$$

Table 1
Isotherm's models applied on atrazine adsorption

Model	Equation	Reference
Langmuir	$q_e = \frac{q_{\max} K_L C_e}{1 + K_L C_e}$ (13)	[38]
	$R_L = \frac{1}{1 + K_L C_0}$ (14)	
	q_{\max} = Maximum adsorption capacity (mg g ⁻¹); C_e = Equilibrium concentration (mg L ⁻¹); K_L = Langmuir's Constant (L mg ⁻¹); C_0 = Initial concentration (mg L ⁻¹); R_L = Langmuir's separation factor; q_e = Equilibrium adsorption capacity (mg g ⁻¹).	
Freundlich	$q_e = K_F C_e^{1/n}$ (15)	[39]
	K_F = Freundlich's Constant (mg g ⁻¹); n = Freundlich's exponent.	
Dubinin–Radushkevich	$\ln(q_e) = \ln(X_m) - k\varepsilon^2$ (16)	[40]
	$\varepsilon = RT \times \ln\left(1 + \frac{1}{C_e}\right)$ (17)	
	$E = \frac{1}{\sqrt{k}}$ (18)	
	X_m = Maximum adsorption capacity (mg g ⁻¹); k = Constant of sorption energy (mol ² J ⁻²); E = Energy of adsorption (J mol ⁻¹); ε = Polanyi's potential; T = Temperature (K); R = Universal gas constant (8.314 J mol ⁻¹ K ⁻¹).	
Polanyi–Manes	$q_e = q_{\max} \exp\left[a \left(RT \times \ln\left(\frac{S_w}{C_e} \right) \right)^b \right]$ (19)	[41]
	a and b = Polanyi's constant; S_w = Solubility of atrazine in water at 298 K (33 mg L ⁻¹).	

The equilibrium isotherms models of Langmuir, Freundlich, Dubinin–Radushkevich, and Polanyi–Manes (Table 1) were fitted to experimental data.

3.4. Thermodynamic study

For neutral or weakly charged adsorbates such as atrazine, the Langmuir's constant can be reasonably approximated to the equilibrium constant and thus be used to obtain the thermodynamic variables of the adsorbent process [42].

As discussed earlier, due to its dependence on the Langmuir's constant temperature K_L was then applied to estimate the changes of the thermodynamic state functions in this study. The parameters evaluated were enthalpy (ΔH), entropy (ΔS), and Gibbs energy (ΔG) and their values were obtained from Eqs. (20) and (21) as follows:

$$\ln(K_C) = \frac{-\Delta G}{RT} \tag{20}$$

$$\ln(K_C) = \frac{\Delta S}{R} - \frac{\Delta H}{RT} \tag{21}$$

where R is the universal gas constant (J mol⁻¹ K⁻¹) and T is the absolute temperature of the system (K).

The equilibrium constant in its nondimensional form, using the constant obtained by fitting the Langmuir model, is represented by Eq. (22) [43]:

$$K_C = MM \times 55.5 \times 1,000 \times K_L \tag{22}$$

where MM is a molecular weight of the adsorbate used (mol g⁻¹); 55.5 is the quantity of moles of pure water in one

liter of solution; 1,000 is the density of pure water, and K_L is the Langmuir's constant ($L\text{ mg}^{-1}$).

3.5. Data analysis

The nonlinear regression of the data, as well as the graphs shown here, was made and modeled using Origin Pro software version 8.0.

4. Results and discussions

4.1. Description

The clay minerals have the characteristic of being expandable, therefore, when adding a host molecule in its structure, we can observe the variation of the basal reflection d_{001} [44]. Given this, XRD becomes an important technique for the evaluation of the structural changes undergone in the preparation stage (chemical synthesis) of the compounds.

Fig. 1 shows the XRD curves obtained for the commercial and organophilic clays. Nondefined peaks are observed,

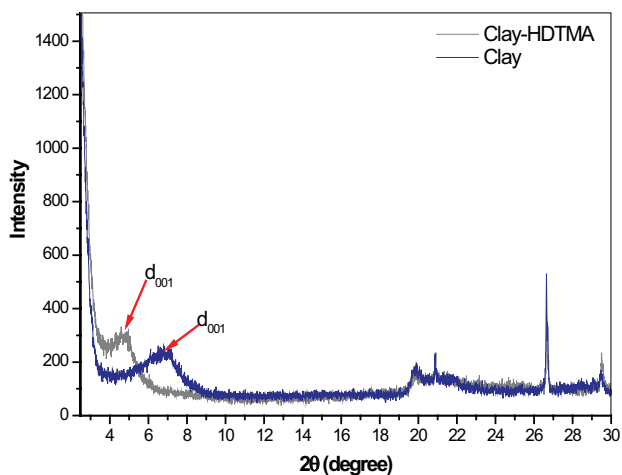


Fig. 1. XDR for organophilic commercial clays.

characterizing that the samples do not have a highly crystalline structure. The peaks detected before $2\theta = 10^\circ$ have a typical wide argilluminous shape [23], with the first reflection at $2\theta = 7.01^\circ$ corresponding to an interlamellar distance of 1,260 pm and, as expected, this distance is increased to 1,828 pm when the HDTMA is interleaved, anticipating the angle to $2\theta = 4.83^\circ$.

The isotherms of adsorption and desorption of nitrogen on the surface of the commercial (a) and organophilic (b) clay are shown in Fig. 2. For commercial Fluidigel clay (Fig. 2(a)), the isotherm found is type IV-b with H4 hysteresis. Type IV isotherms are attributed to mesoporous adsorbents often found in mesoporous oxides, industrial adsorbents, and mesoporous molecular sieves. H4 hysteresis is related to mesoporous adsorbents as well. Examples are compounds such as aggregated crystals of zeolites, mesoporous zeolites, and microporous carbons [45].

After the chemical modification, the organophilic clay (Fig. 2(b)) started to present type II isotherm, which characterizes an adsorbent with a macroporous or nonporous compounds [45].

Table 2 presents the values of specific area and average pore volume of the clays found by N_2 fission analysis. The organophilic clay has a smaller area and volume of pores when compared with the commercial. This decrease is related to the fact that the surfactant prevents the adsorption of the nitrogen molecules on the surface of the material, thus reducing their respective values of pore area and volume, confirming the insertion of the cationic salt in the interplanar spaces of the clayey [44].

Through the identification of the chemical compounds (Fig. 3), we observed the presence of the groups OH, which correspond to the stretches $3,629$ and $1,623\text{ cm}^{-1}$, characteristic deformities of the groups SiO in the regions of 793 and $1,036\text{ cm}^{-1}$, of the groups Si_2O and $AlOSi$, detected in 467 and 530 cm^{-1} [30], and we also noted H_2O in the band of $3,449\text{ cm}^{-1}$ [30], in both of the samples. However, the pair of bands in the range of $2,848$ and $2,942\text{ cm}^{-1}$ that appears only for the modified clay is due to the vibrations of the asymmetrical and

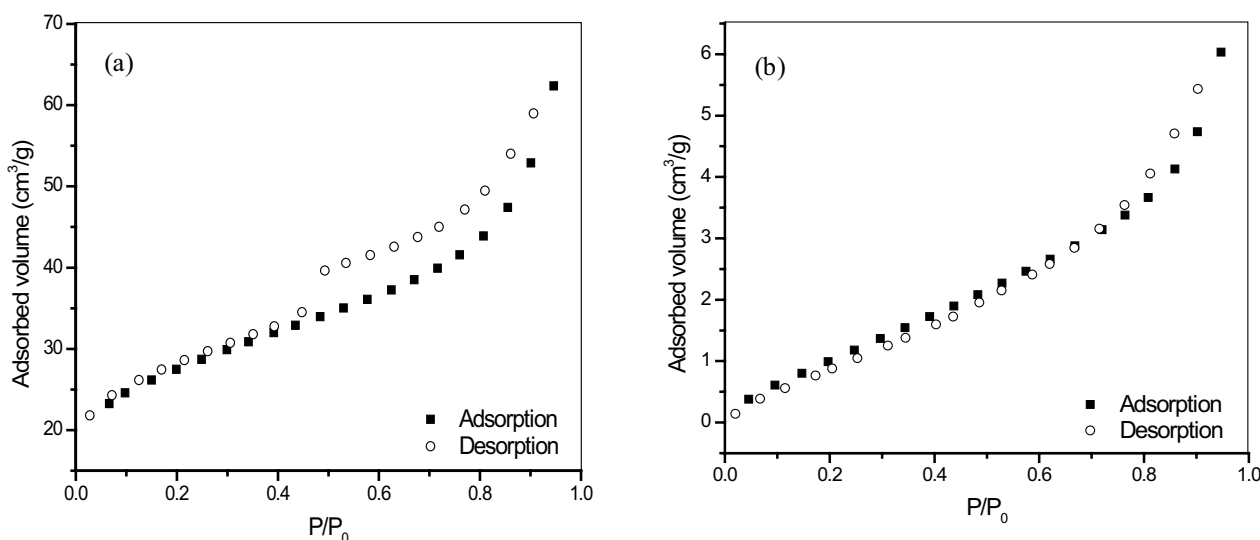


Fig. 2. N_2 adsorption and desorption isotherms for (a) commercial Fluidigel clay and (b) organophilic clay.

Table 2
Specific area and pore volume of commercial and organophilic clays

Clay	S_g ($m^2 g^{-1}$)	V_p ($cm^3 g^{-1}$)
Commercial	91.3	0.09645
Organophilic	5.3	0.00933

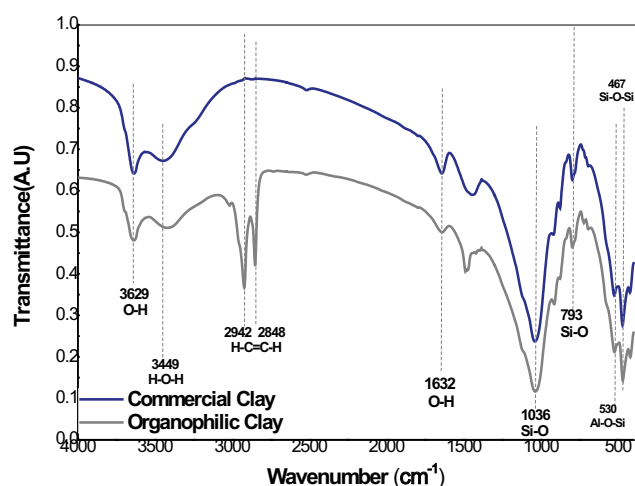
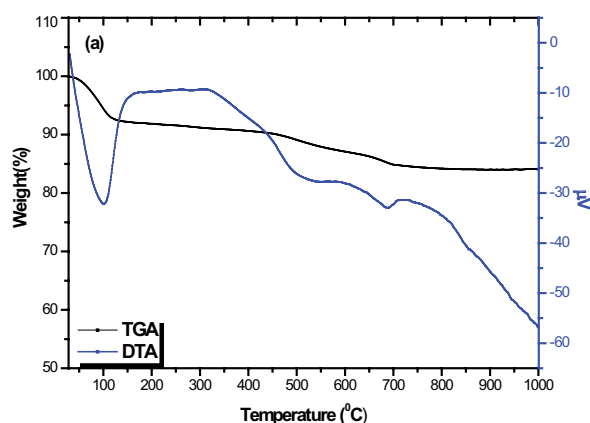


Fig. 3. FTIR for commercial and organophilic clays.

symmetrical stretches from the group CH_2 from the organic component in the chemical synthesis stage [26].

The DTA curve (Fig. 4(a)) for the commercial clay shows an endothermic peak at $100^\circ C$, which corresponds to the loss of water intercalated and adsorbed in its structure [30]. It is also noted the presence of two other endothermic peaks, one at $530^\circ C$ caused by the loss of structural hydroxyls and another at $690^\circ C$ referring to the destruction of the crystalline reticulum [46]. The decline of the curve at around $800^\circ C$ indicates the fusion of the material [47].

On the other hand, from the TGA (Fig. 3(a)), it is possible to perceive two regions of mass loss; the first one until approximately $130^\circ C$ assigned to free water and the second one to $700^\circ C$, referring to the structural loss, thus obtaining a total of 15.87% mass loss for the commercial clay [46].



After the chemical modification (Fig. 4(b)), the clay shows an exothermic peak in the temperature region between $250^\circ C$ and $480^\circ C$, which is attributed to the decomposition of the HDTMA, after the phase of release of the water that was adsorbed physically [46]. In the region between $650^\circ C$ and $900^\circ C$, there are two endothermic peaks; the first one due to the decomposition of the residual salt and the second one to the combustion of carbonaceous residues [46].

The TGA for the clay Fluidgel organophilic (Fig. 3(b)) shows three regions of mass loss, the first inflection occurs until approximately $100^\circ C$, which corresponds to the adsorbed free water, the second one up to $420^\circ C$, related to the initial decomposition of the organic salt, and the third one until $730^\circ C$ for the final salt decomposition [46].

Thus, the total mass loss, from room temperature to $1,000^\circ C$, was of approximately 35.2% for the chemically modified compound.

From the images obtained by SEM (Fig. 5), it was not possible to observe, in the analyzed magnification (increase of 5,000 times), the presence of pores in both the commercially (Fig. 4(a)) and chemically modified clay (Fig. 5(b)). However, we can see the heterogeneity of the surface of the materials, according to studies by Cantuaria et al. [30], which uses Verde-Lodo clay in the adsorption of silver.

The semiquantitative chemical analyzes determined by EDX for the commercial and organophilic Fluidgel clays are shown in Table 3. It is noted that the commercial Fluidgel clay consists basically of silicon, oxygen, iron, and aluminum. These compounds are the main chemical constituents of the clay minerals belonging to the group of smectites [26].

After the organophilization stage, the absence of sodium and the appearance of carbon in the chemical composition of the mineral are verified (Table 3). Due to the cation exchange from the chemical synthesis, the sodium cation previously present in the sample was replaced by the alkyl ammonium cations of the quaternary salt. This fact also points out that the organophilization stage of the clay was actually successfully performed via the chemical synthesis process.

4.2. Effect of pH and dosage of adsorbent on the removal of atrazine

To analyze the influence of pH on the removal of atrazine by the organoclay, experiments were performed varying the

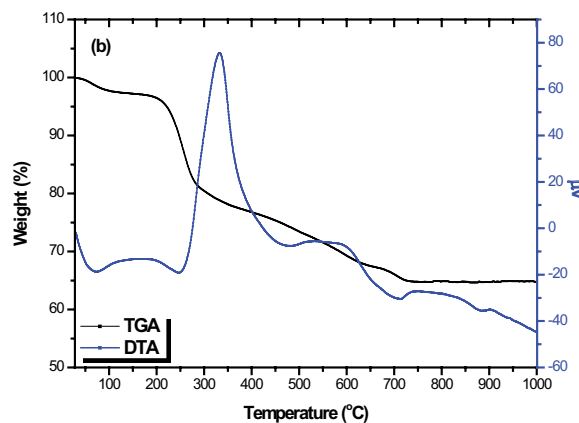


Fig. 4. TGA/DTA for clays (a) commercial and (b) organophilic.

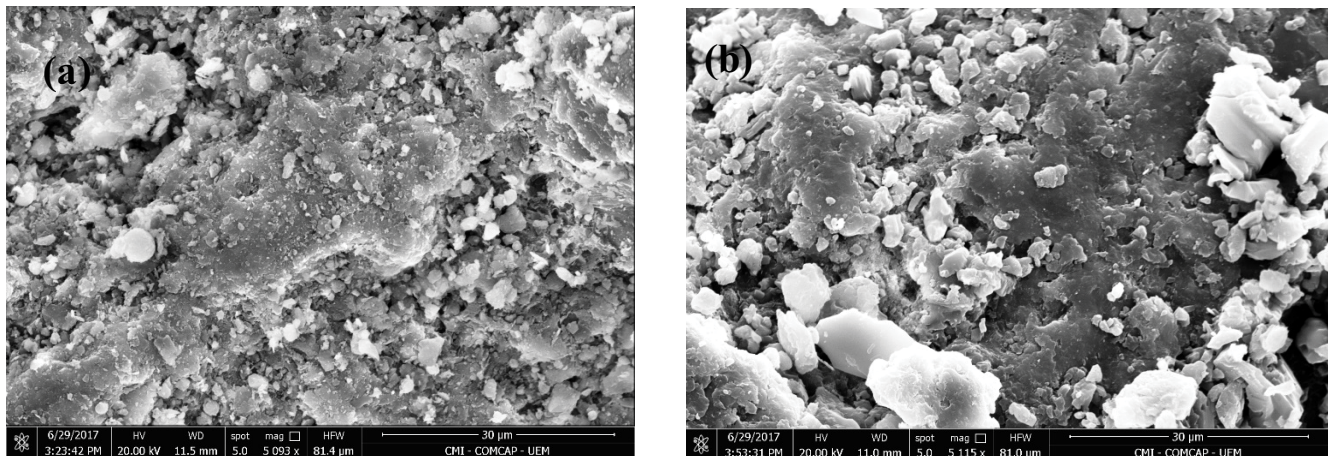


Fig. 5. SEM for commercial (a) and (b) organophilic clay.

Table 3
EDX analysis for commercial and organophilic clays

Chemical element	O	Si	Au	Fe	Al	Ca	Na	Mg	C
Fluidgel commercial	44.2	24.5	9.3	8.8	7.0	2.9	1.6	1.6	0
Fluidgel organophilic	28.3	13.0	11.0	3.9	6.9	1.0	0	1.0	35.0

initial pH of the solution in values of 2–12 (Fig. 6(a)). It is observed that the removal of the contaminant is little dependent on the pH in this range. Removal decreases slightly at pH = 2 and pH = 12, which may indicate a desorption process at these values. Although pH is an important variable in adsorption, it has not been shown to be as significant in the removal of atrazine. These results are similar to those obtained by Santos et al. [48], who investigated the adsorption capacity of synthetic orange dye using organophilic clay. The low pH influence on atrazine adsorption is also justified by its pK_a value (1.7). The atrazine has a basic character and at pH values higher than the value of its pK_a the molecule has

a neutral charge. The ionization of possible oxygen groups on the clay surface will not contribute to the adsorption of adsorbate and adsorbate in this pH range (2–12).

However, according to Fig. 6(b), we verified that the removal rate increases as the amount of adsorbent expands in the system. This fact can probably be correlated to the larger area available to the adsorption of the herbicide in the material solid surface [49]. Coldebella et al. [2] found the same behavior on biosorption of atrazine in the oleander moringa Lam bark, where the best removal was achieved with higher dosages of adsorbent. We obtained in the optimized conditions of this study a removal of 61.37% of atrazine. In fact,

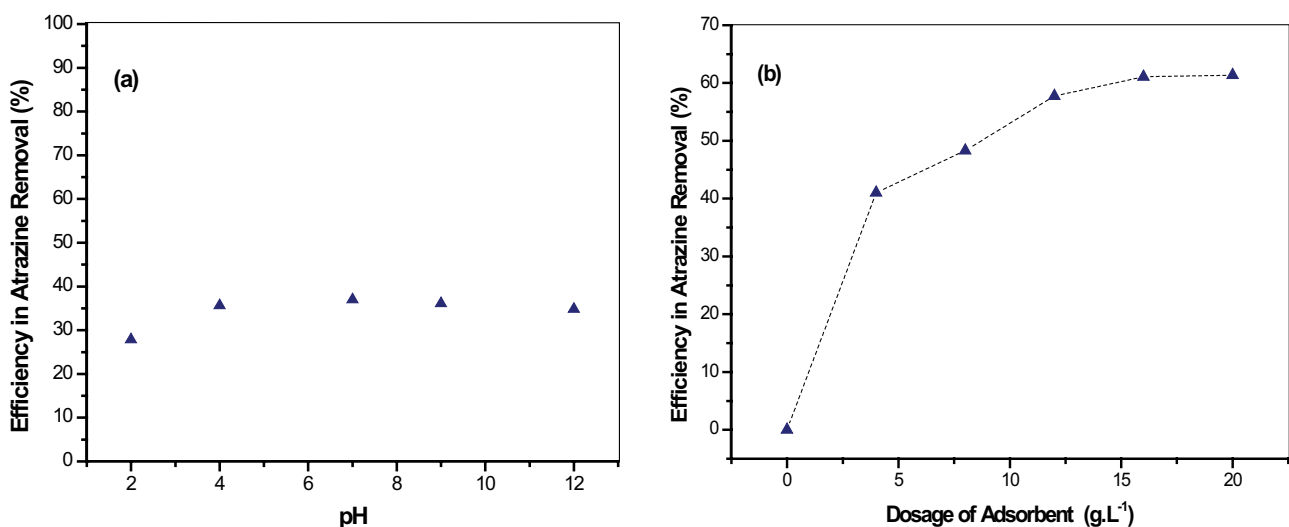


Fig. 6. Study of the effect of (a) pH and (b) dosage of adsorbent on atrazine adsorption.

results between 56% and 63% were found in the removal of atrazine by using vermiculite organophilic clay as well as by using the diatomaceous dirty (up to 55%) [50,51].

4.3. Time of contact

Fig. 7 shows the kinetic data, where Elovich's equation was the model that better represented the profiles of concentration (see Table 4).

Elovich assumes that the materials that have surfaces composed of energetically heterogeneous sites, which the process of desorption as well as the species involved in the system do not influence in a significant way in the Kinect adsorption [52].

However, as much as Elovich's equation has better fitted the experimental values, it does not allow clarifying information concerning adsorption mechanisms. Several processes can influence the kinetic rate, among them we can point the external diffusion, in the boundary layer and intraparticle [2]. In this case, the intraparticle diffusion model was used to better understand the kinetic steps in the process.

It is possible to observe in Fig. 8 three stages of adsorption, each one involving a different step in the adsorbent process:

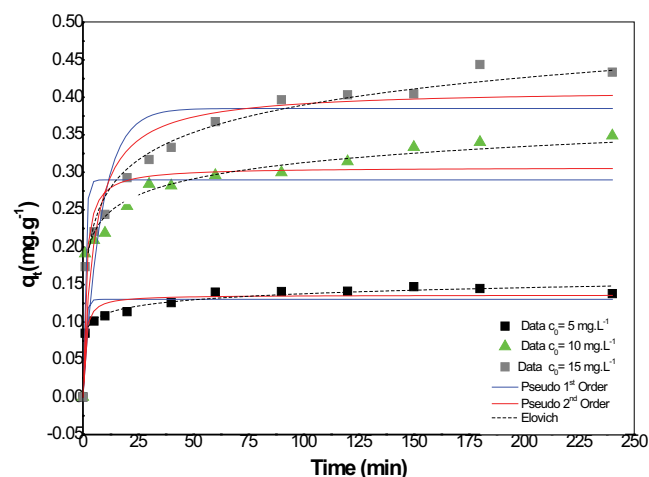


Fig. 7. Adjustment to kinetic adsorption models.

Table 4
Data of the adjusted kinetic models

Model	Parameters	C_0 (mg L ⁻¹)	C_0 (mg L ⁻¹)	C_0 (mg L ⁻¹)
		5	10	15
Pseudo-first-order model	k_1 (min ⁻¹)	1.002	1	0.110
	q_e (mg g ⁻¹)	0.13	0.29	0.392
	R^2	0.858	0.772	0.8
Pseudo-second-order model	k_2 (g mg ⁻¹ min ⁻¹)	7.987	2.65	0.451
	q_e (mg g ⁻¹)	0.136	0.34	0.417
	R^2	0.923	0.862	0.895
Elovich's model	a (mg g ⁻¹ min ⁻¹)	14.47	6.8	0.83
	b (g mg ⁻¹)	85.05	32.01	18.88
	R^2	0.986	0.984	0.986

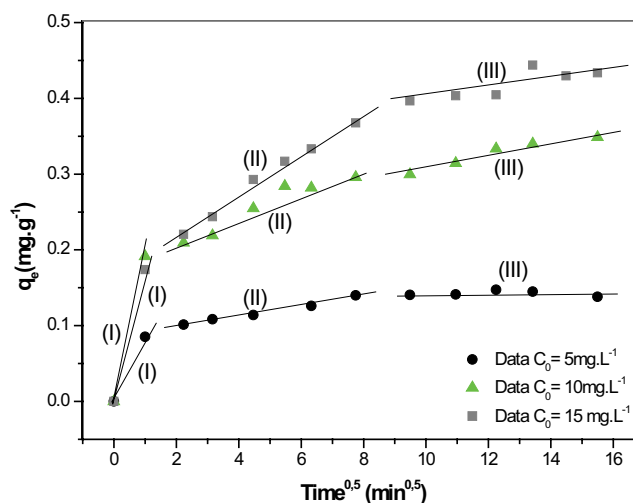


Fig. 8. Intraparticle diffusion kinetics for atrazine adsorption.

the first region ($0 < t^{1/2} < 1$) of rapid onset and linear characteristic which corresponds to a step controlled by external transport. This step is related to the time spent by the organic molecule as it diffuses from the sinus of the fluid phase to the surface of the adsorbent particle. The second region ($1 < t^{1/2} < 8$) concerns intraparticle diffusion effects. Generally, high porosity solids have a considerable amount of micropores, which may hinder the mobility of high-molecular-mass adsorbates within the adsorbent material. These intraparticle diffusion effects may be intricately linked to a reduction in adsorption velocity and consequently an increase in process time. The third region ($8 < t^{1/2} < 16$) is the final stage, in which one can perceive the decrease of intraparticle diffusion effects due to the reach of the dynamic equilibrium in the system [53].

Fig. 9 shows the adjustments of the three concentration profiles for Boyd's model. The coefficient of effective diffusivity D_i (cm² min⁻¹) for each concentration was determined with the angular coefficient obtained from the linear regression.

The kinetic constants for intraparticle diffusion and Boyd's models are shown in Table 5, and in both the cases, there was no interception of the two models in the system's

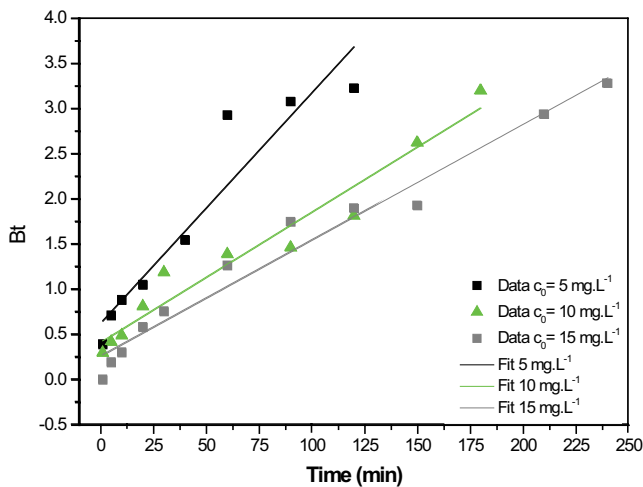


Fig. 9. Linear adjustment of the Boyd's model.

origin. This fact indicates that the process limit stage was not the interparticle diffusion but the film diffusion. When compared the values of k_i and D_r , both grow as the adsorbate initial concentration is increased, this is attributed to the fact that the solution is more concentrated, which enables the molecules access to the material active sites.

In the literature, diffusion coefficient values are reported in the same order of objectives in the study by Freitas et al. [54] that obtained values in the order of 10^{-6} for an adsorption of the copper and silver ions in Verde-lodo bentonite clay. There are also values of kinetic studies with atrazine using organophilic modified clay with the cationic surfactant octadecyl trimethyl ammonium bromide, in which values of adsorption capacity of 0.3 mg g^{-1} were reached at a concentration of 10 mg L^{-1} [55]. With Fluidigel clay used in this study modified with HDTMA to the same concentration, it was obtained a very similar value of 0.34 mg of atrazine per gram of adsorbent.

4.4. Equilibrium

As observed from Fig. 10, we might notice that, with the increase of adsorbate concentration, the adsorption capacity growth was verified at the three temperatures used. This is explained due to the increased concentration gradient of the system. As the solution is richer in atrazine molecules, this phenomenon facilitates the transport of the contaminant that lies in the fluid region to the surface of the material, which

contributes to the access of them to the active sites of the adsorbent.

In order to evaluate equilibrium and superficial characteristics, several isothermal equations used in gas phase adsorption can be approximated to equilibrium in liquid phase for a single component [56]. Table 6 presents the results of the adjustments applied in this study. The Polanyi–Manes equation was the one that best represented the data in the three temperatures evaluated. This model assumes an energetically heterogeneous surface in which when a molecule is inside an attractive field of a solid, there will be an adsorption potential between the molecule and the solid surface of the adsorbent [41]. This fact contributes with the analyses of contact time (adsorption kinetics) performed in this research, in which heterogeneous surface characteristics proposed by the Elovich's model were verified, adjusted to the contact time test (better kinetic fit).

The dimensionless factor of Langmuir provides subsidies to understand the type of isotherm, favorable ($R_L < 1$), linear ($R_L = 1$), or unfavorable ($R_L > 1$) obtained from experiments. The adsorption of atrazine was favorable in the three evaluated temperatures and with considerably low values, reporting good affinity between the components.

Parameter values in Freundlich's equation reinforce the analysis made by the Langmuir R_L parameter. Values of $n > 1$ were obtained in the three experimental conditions investigated and that strengthened a favorable feature of the process [57].

The magnitude of E (kJ mol^{-1}) estimated by the Dubinin–Radushkevich's model was used to understand the nature of the adsorption. If the process is physical, the average adsorption energy values are below 8 kJ mol^{-1} and in fact this is observed when analyzing Table 6 [58]. It is found values below the range of energy mentioned, confirming an adsorption of physical nature.

Although the Polanyi–Manes's model was the best fit, the one proposed by Langmuir is still the most used in the literature to compare the adsorption capacity between materials. Table 7 shows other studies aimed at the removal of atrazine from contaminated water, and organophilic clay was the one that showed the best performance, indicating that it is a promising material in the removal of these contaminants from wastewater.

4.5. Thermodynamics

The values of enthalpy and adsorption entropy were calculated stem from the graphic confection of $\text{Ln}(K_c) \times 1/T$ (K^{-1}),

Table 5
Intraparticle and Boyd diffusion settings data

Model	Parameter	C_0 (mg L^{-1})	C_0 (mg L^{-1})	C_0 (mg L^{-1})
		5	10	15
Intraparticle diffusion model	K ($\text{mg g}^{-1} \text{min}^{-0.5}$)	0.032	0.077	0.108
	C (mg g^{-1})	0.039	0.071	0.047
	R^2	0.813	0.889	0.963
Boyd's model	D_i ($\text{cm}^2 \text{min}^{-1}$)	4.723×10^{-6}	2.675×10^{-6}	2.384×10^{-6}
	R^2	0.885	0.949	0.967

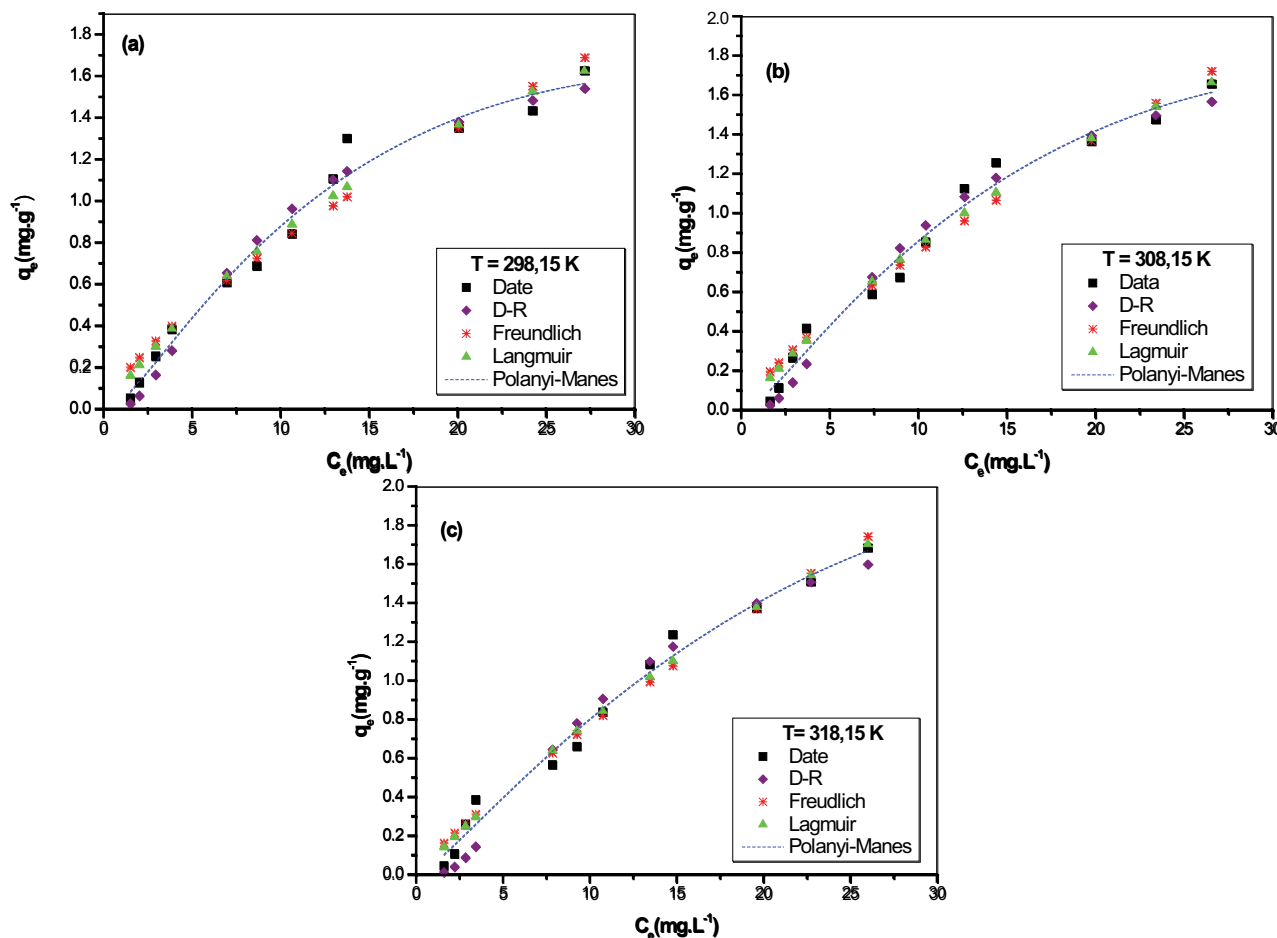


Fig. 10. Equilibrium isotherms for the adsorption of atrazine in organophilic clays at temperatures (a) 298 K, (b) 308 K, and (c) 318 K.

Table 6
Models adjusted for equilibrium isotherms

Model	Parameter	Temperature		
		T = 25°C	T = 35°C	T = 45°C
Langmuir	q_{max} (mg g ⁻¹)	3.492	4.136	6.060
	K_L (L mg ⁻¹)	0.032	0.025	0.015
	R_L	0.342	0.397	0.526
	R^2	0.966	0.972	0.980
Freundlich	K_f (L mg ⁻¹)	0.146	0.132	0.107
	n	1.350	1.278	1.171
	R^2	0.947	0.975	0.975
Dubinin–Radushkevich (D–R)	X_m (mg g ⁻¹)	2.113	2.213	2.427
	k (mol ² J ⁻²)	0.003	0.003	0.004
	E (kJ mol ⁻¹)	0.017	0.016	0.015
	R^2	0.969	0.965	0.959
Polanyi–Manes	q_{max} (mg g ⁻¹)	1.610	1.694	1.836
	a	–0.002	–0.003	–0.008
	B	1.671	1.540	1.341
	R^2	0.976	0.978	0.982

Table 7
Comparison of organophilic clay with other adsorbents

Adsorbent	q_{max} (mg g ⁻¹)	Reference
Organophilic clay	3.492	This study
Coal Ash	3.330	[59]
Zeolite X	4.779	[60]
Nanocomposite of Fe-Zr-Mn	0.300	[61]
Zeolite Organomodifies	0.431	[62]
Wood Charcoal	0.800	[63]

as exhibited in Fig. 11. The values of Gibbs energy for each temperature as well as the enthalpy and adsorption entropy are shown in Table 8.

The negative enthalpy suggests exothermic nature in the process. In thermodynamics standpoint the heat involved in the physisorption generally is located in about 20 kJ mol⁻¹, that is, of a condensation/vaporization order, whereas the chemisorption heat is of an order of reaction heat, approximately 200 kJ mol⁻¹ [64]. In this work, it was obtained the enthalpy value of –29.7 kJ mol⁻¹, which is in the order of the values for physisorption confirming the physical nature of the process. In terms of entropy, it was observed positive

Table 8
Thermodynamic parameters for adsorption of atrazine in organophilic clay

Temperature (K)	1/T (K ⁻¹)	K _c ·10 ⁻³	ΔG (kJ mol ⁻¹)	ΔH (kJ mol ⁻¹)	ΔS (J mol ⁻¹ K ⁻¹)	R ²
298	0.0033	383.08	-31.85			
308	0.0032	299.28	-32.29	-29.72	7.52	0.91
318	0.0031	179.57	-31.98			

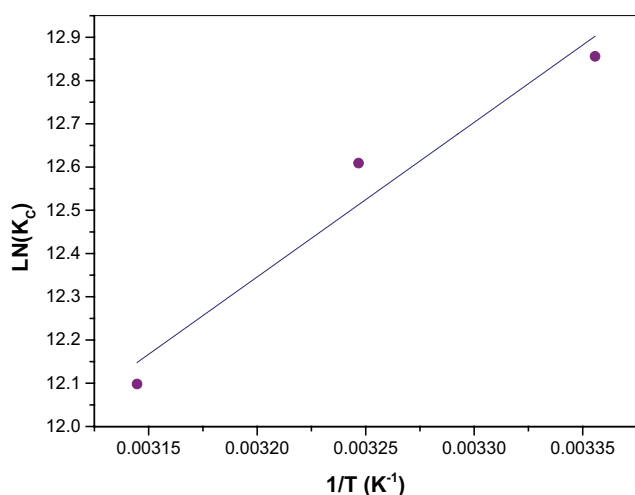


Fig. 11. Variation of the equilibrium constant at different temperatures.

values, which indicates that randomness is increased in the process.

Negative values of enthalpy are mentioned in literature, as well as in the usage of carbon nanotubes for atrazine adsorption, once it was found value of ΔH equal to $-28.69 \text{ kJ mol}^{-1}$, and also in silver and chrome adsorption in bentonite clay [65,66].

Negative values of ΔG indicate spontaneity in the process and its magnitude can be also used to verify whether the process is controlled by physical (-20 to 0 kJ mol^{-1}) or chemical adsorption (values around -400 to -80 kJ mol^{-1}) [67]. For this study, we verified that when ΔG values are compared in the three temperatures, both are very close to the physisorption range. These values reinforce the considerations made by the nature of the process with the other thermodynamic parameters analyzed in this study such as enthalpy and adsorption energy (obtained by the Dubinin–Radushkevich equation).

5. Conclusion

The chemical treatment of the commercial Fluidgel clay with HDTMA was efficient in the organic clay production. The physisorption analyses of N_2 , TGA/DTA, XDR, FTIR, and EDX demonstrate that textural, thermic, structural, and chemical modifications occurred in the surface of the compound after the chemical synthesis, validating the organophilization process of this material.

The organic clay presented a great performance when applied in water treatments containing atrazine, with removal of 61.37% and maximum adsorption capacity

of 3.492 mg g^{-1} . The kinetic model that best depicted the experimental values was the Elovich's equation and it was verified by the mechanistic attitude of adsorption that the intraparticle step was not the bounding stage. From equilibrium study, Polanyi–Manes isotherm was the one which presented the best correlation and the thermodynamics study indicated physisorption and process of exothermic nature.

Acknowledgments

The authors express thankfulness to CAPES (Coordenação de Aperfeiçoamento de Pessoal de Nível Superior), CNPQ (Conselho Nacional de Desenvolvimento Científico e Tecnológico), COMCAP (Complexo de Centrais de Apoio a Pesquisa), UEM (Universidade Estadual de Maringá), and UNICAMP (Universidade Estadual de Campinas).

References

- [1] M. Petrovic, S. Gonzalez, D. Barcelo, Analysis and removal of emerging contaminants in wastewater and drinking water, *Trends Anal. Chem.*, 22 (2013) 685–696.
- [2] P.F. Coldebella, M.R.F. Klen, L. Nishi, K.C. Valverde, E.B. Cavalcanti, O.A.A. dos Santos, R. Bergamasco, Potential effect of chemical and thermal treatment on the kinetics, equilibrium, and thermodynamic studies for atrazine biosorption by the *Moringa oleifera* pods, *Can. J. Chem. Eng.*, 95 (2016) 961–973.
- [3] S.M. Alshehri, M. Naushad, T. Ahamad, Z.A. Allothman, A. Aldalbahi, Synthesis, characterization of curcumin based ecofriendly antimicrobial bioadsorbent for the removal of phenol from aqueous medium, *Chem. Eng. J.*, 254 (2014) 181–189.
- [4] A.A. Alqadami, M. Naushad, M.A. Abdalla, M.R. Khan, Z.A. Allothman, Adsorptive removal of toxic dye using Fe₃O₄-TSC nanocomposite: equilibrium, kinetic, and thermodynamic studies, *J. Chem. Eng. Data*, 61 (2016) 3806–3813.
- [5] A.B. Albadarin, M. Charara, B.M.A. Tarboush, M.N.M. Ahmad, T.A. Kurniawan, M. Naushad, G.M. Walker, C. Mangwandi, Mechanism analysis of tartrazine biosorption onto masau stones; a low cost by-product from semi-arid regions, *J. Mol. Liq.*, 242 (2017) 478–483.
- [6] M. Naushad, Z.A. Allothman, M.R. Awual, S.M. Alfadul, T. Ahamad, Adsorption of rose Bengal dye from aqueous solution by amberlite Ira-938 resin: kinetics, isotherms, and thermodynamic studies, *Desal. Wat. Treat.*, 57 (2015) 13527–13533.
- [7] R.J. Gilliom, J.E. Barbash, C.G. Crawford, P.A. Hamilton, J.D. Martin, N. Nakagaki, L.H. Nowell, J.C. Scott, P.E. Stackelberg, G.P. Thelin, D.M. Wolock, *Pesticides in the Nation's Streams and Ground Water, 1992–2001*, 3rd ed., USGS, Virginia, 2006.
- [8] N.W. Brown, E.P.L. Roberts, A. Chasiotis, T. Cherdron, N. Sanghrajka, Atrazine removal using adsorption and electrochemical regeneration, *Water Res.*, 38 (2004) 3067–3074.
- [9] Sindag, Mercado Brasileiro de Fitossanitários. Apresentado no Workshop Avaliação da Exposição de Misturadores, Abastecedores e Aplicadores a Agrotóxicos, 2009.

- [10] F.F. Carneiro, R.M. Rigotto, L.G. S. Augusto, K. Friedrich, A.C. Búrigo, Dossiê ABRASCO: Um alerta sobre os impactos dos agrotóxicos na saúde, 1st ed., Expressão Popular, São Paulo, 2015. http://www.abrasco.org.br/dossieagrototoxicos/wp-content/uploads/2013/10/DossieAbrasco_2015_web.pdf.
- [11] A.M.C. Barbosa, M.de L.M. Solano, G.de A. Umbuzeiro, Pesticides in Drinking Water – The Brazilian Monitoring Program, *Front Public Heal.*, 3 (2015) 1–10.
- [12] E.C. Bortoluzzi, D.S. Rheinheimer, C.S. Gonçalves, J.B.R. Pellegrini, A.M. Maroneze, M.H.S. Kurz, N.M. Bacar, R. Zanella, Investigation of the occurrence of pesticide residues in rural wells and surface water following application to tobacco, *Quim. Nova*, 30 (2007) 1872–1876.
- [13] R. Freire, R.M. Schneider, F.H. de Freitas, C.M. Bonifácio, C.R.G. Tavares, Monitoring of toxic chemical in the basin of Maringá stream, *Acta Sci.*, 34 (2012) 295–302.
- [14] J.C. Moreira, F. Peres, A.C. Simões, W.A. Pignati, E.de C. Dores, S.N. Vieira, C. Strüssmann, T. Mott, Contaminação de águas superficiais e de chuva por agrotóxicos em uma região do estado do Mato Grosso, *Ciência E Saúde Coletiva*, 17 (2012) 1557–1568.
- [15] E.W.C. Steinberg, R. Lorenz, H. Spieser, Effects of atrazine on swimming behavior of zebrafish, *Brachydanio rerio*, *Rapid Commun.*, 29 (1995) 981–985.
- [16] J.P. Lasserre, F. Fack, D. Revets, S. Planchon, J. Renaut, L. Hoffmann, A.C. Gutleb, C.P. Muller, T. Bohn, Effects of the endocrine disruptors atrazine and PCB 153 on the protein expression of MCF-7 human cells, *J. Proteome Res.*, 30 (2009) 5485–5496.
- [17] D.E. Tillitt, D.M. Papoulias, J.J. Whyte, C.A. Richter, Atrazine reduces reproduction in fathead minnow (*Pimephales promelas*), *Aquat. Toxicol.*, 99 (2010) 149–159.
- [18] C. Hao, A. Gely-Pernot, C. Kervarrec, M. Boudjema, E. Becker, P. Khil, S. Tevosian, B. Jegou, F. Smagulova, Exposure to the widely used herbicide atrazine results in deregulation of global tissue-specific RNA transcription in the third generation and is associated with a global decrease of histone trimethylation in mice, *Nucl. Acids Res.*, 44 (2016) 9784–9802.
- [19] E. European Union, Directive 2008/105/EC of the European Parliament and of the Council of 16 December 2008 on environmental quality standards in the field of water policy, 2008.
- [20] M.da S.do Brasil, Portaria N° 2.914, DE 12 DE DEZEMBRO DE 2011, Ministério Da Saúde, 2011. <http://bvsms.saude.gov.br/bvs/saudelegis/gm/2011/p>.
- [21] F.B. Scheufele, A.N. Módenes, C.E. Borba, C. Ribeiro, F.R. Espinoza-Quiñones, R. Bergamasco, N.C. Pereira, Monolayer-multilayer adsorption phenomenological model: kinetics, equilibrium and thermodynamics, *Chem. Eng. J.*, 284 (2016) 1328–1341.
- [22] C. Bertagnolli, S.J. Kleinübing, M.G.C. da Silva, Preparation and characterization of a Brazilian bentonite clay for removal of copper in porous beds, *Appl. Clay Sci.*, 53 (2013) 73–79.
- [23] C. Bertagnolli, M.G.C. da Silva, Characterization of Brazilian bentonite organoclays as sorbents of petroleum-derived fuels, *Mater. Res.*, 15 (2012) 253–259.
- [24] S. Bedin, M.F. Oliveira, M.G.A. Vieira, O.A.A. dos Santos, M.C.G. da Silva, Adsorption of toluene in batch system in natural clay and organoclay, *Chem. Eng. Trans.*, 32 (2013) 313–318.
- [25] Y. Seki, K. Yurdaoç, Paraquat adsorption onto clays and organoclays from aqueous solution, *J. Colloid Interface Sci.*, 287 (2005) 1–5.
- [26] R. Barbosa, E.M. Araújo, A.D. de Oliveira, T.J.A. de Melo, Effect of quaternary ammonium salts on the organophilization of national bentonite clay, *Cerâmica*, 52 (2006) 264–268.
- [27] P.M. Naranjo, J. Molina, E.L. Sham, E.M.F. Torresa, Synthesis and characterization of HDTMA-organoclays: insights into their structural properties, *Quim. Nova*, 38 (2015) 166–171.
- [28] S. Brunauer, P.H. Emmett, E. Teller, Adsorption of gases in multimolecular layers, *J. Am. Chem. Soc.*, 60 (1938) 309–319.
- [29] E.P. Barrett, L.G. Joyner, P.P. Halenda, The determination of pore volume and area distributions in porous substances. I. Computations from nitrogen isotherms, *J. Am. Chem. Soc.*, 73 (1951) 373–380.
- [30] M.L. Cantuaria, A. osio F. de A. Neto, E.S. Nascimento, M.G.A. Vieira, Adsorption of silver from aqueous solution onto pre-treated bentonite clay: complete batch system evaluation, *J. Clean. Prod.*, 112 (2015) 1–10.
- [31] N. Lu, S.M. Chen, J.Y. Chen, C.Y. Yang, Y.P. Yeh, T.Y. Feng, Y. Shih, T. Kokulnathan, D. Chen, Enhanced photocatalytic degradation of atrazine by platinized titanium dioxide under 352 nm irradiation, *Water Sci. Technol.*, 75 (2016) 1–11.
- [32] S.Y. Lagergren, Zur Theorie der sogenannten Adsorption gelöster Stoffe Kungliga Svenska Vetenskapsakademiens, *Handlingar*, 24 (1898) 1–39.
- [33] Y. Ho, G. McKay, A comparison of chemisorption kinetic models applied to pollutant removal on various sorbents, *Process Saf. Environ. Prot.*, 76 (1998) 332–340.
- [34] C. Aharoni, F.C. Tompkins, Kinetics of adsorption and desorption and the Elovich equation, *Adv. Catal.*, 21 (1970) 1–49.
- [35] W. Weber, J.C. Morris, Kinetics of adsorption on carbon from solution, *J. Sanit. Eng. Div. (Proc. ASCE)*, 89 (1963) 31–59.
- [36] G. Boyd, A.W. Adamson, L.S.M. Jr., The exchange adsorption of ions from aqueous solutions by organic zeolites, *J. Am. Chem. Soc.*, 69 (1947) 2836–2848.
- [37] D. Reichenberg, Properties of ion-exchange resins in relation to their structure. III. Kinetics of exchange, *J. Am. Chem. Soc.*, 75 (1953) 589–597.
- [38] I. Langmuir, The constitution and fundamental properties of solids and liquids. Part I. Solids, *J. Am. Chem. Soc.*, 38 (1916) 2221–2295.
- [39] H.M.F. Freundlich, Over the adsorption in solution, *J. Phys. Chem.*, 57 (1926) 385–471.
- [40] M. Dubinin, L. Radushkevich, The equation of the characteristic curve of activated charcoal, *Acad. Sci. Phys. Chem.*, 55 (1947) 331.
- [41] M. Polanyi, The potential theory of adsorption, *Science*, 141 (1963) 1010–1013.
- [42] Y. Liu, Is the free energy change of adsorption correctly calculated?, *J. Chem. Eng. Data*, 54 (2009) 1981–1985.
- [43] H.N. Tran, S.J. You, H.P. Chao, Thermodynamic parameters of cadmium adsorption onto orange peel calculated from various methods: a comparison study, *J. Environ. Chem. Eng.*, 4 (2016) 2671–2682.
- [44] C.W. Lopes, F.G. Penha, R.M. Braga, D.M. de A. Melo, S.B.C. Pergher, D.I. Petkowicz, Síntese e caracterização de argilas organofílicas contendo diferentes teores do surfactante catiônico brometo de hexadeciltrimetilamônio, *Quim. Nova*, 34 (2011) 1152–1156.
- [45] M. Thommes, K. Kaneko, A.V. Neimark, J.P. Olivier, F. Rodriguez-Reinos, J. Rouquerol, K.S.W. Sing, Physisorption of gases, with special reference to the evaluation of surface area and pore size distribution (IUPAC Technical Report), *Pure Appl. Chem.*, 87 (2015) 1051–1069.
- [46] S.B. Cabral, S.C.G. Rodrigues, K.R.O. Pereira, F.R. Valenzuela-Díaz, F.M.G. Rodrigues, Síntese e caracterização de argila organofílica visando sua utilização como adsorvente na remoção de cromo, *Rev. Eletrônica Mater. E Process*, 4 (2009) 21–28.
- [47] P. de S. Santos, Tecnologia de argilas aplicada às argilas brasileiras: Aplicações, 1st ed., Edgard Blucher, São Paulo, 1975.
- [48] O.A.A. dos Santos, C.Z. Castelli, M.F. Oliveira, A.F. de A. Neto, M.G.C. da Silva, Adsorption of synthetic orange dye wastewater in organoclay, *Chem. Eng. Trans.*, 32 (2013) 307–312.
- [49] S.P. Raghuvanshi, R. Singh, C.P. Kaushik, Kinetics study of methylene blue dye bioadsorption on baggase, *Appl. Écol. Environ. Res.*, 2 (2004) 35–42.
- [50] G. Abate, J.C. Masini, Sorption of atrazine, propazine, deethylatrazine, deisopropylatrazine and hydroxyatrazine onto organovermiculite, *J. Braz. Chem. Soc.*, 16 (2005) 936–943.
- [51] K. Agdi, A. Bouaid, A.M. Esteban, P.F. Hernando, A. Azmania, C. Camara, Removal of atrazine and four organophosphorus pesticides from environmental waters by diatomaceous earthremediation method, *R. Soc. Chem.*, 2 (2000) 420–423.

- [52] S. Sen Gupta, K.G. Bhattacharyya, Kinetics of adsorption of metal ions on inorganic materials: a review, *Adv. Colloid Interface Sci.*, 162 (2011) 39–58.
- [53] I.A. Tan, A.L. Ahmad, B. Hameed, Adsorption isotherms, kinetics, thermodynamics and desorption studies of 2,4,6-trichlorophenol on oil palm empty fruit bunch-based activated carbon, *J. Hazard. Mater.*, 164 (2009) 473–482.
- [54] E.D. Freitas, A.C.R. Carmo, A.F.A. Neto, M.G.A. Vieira, Binary adsorption of silver and copper on Verde-lodo bentonite: kinetic and equilibrium study, *Appl. Clay Sci.*, 137 (2017) 69–76.
- [55] E. Grundgeiger, Y.H. Lim, R.L. Frost, G.A. Ayoko, Y. Xi, Application of organo-beidellites for the adsorption of atrazine, *Appl. Clay Sci.*, 105–106 (2015) 252–258.
- [56] H. Hindarso, S. Ismadji, F. Wicaksana, A. Mudjijati, N. Indraswati, Adsorption of benzene and toluene from aqueous solution onto granular activated carbon, *J. Chem. Eng.*, 46 (2001) 788–791.
- [57] A.M. Aljeboree, A.N. Alshirifi, A.F. Alkaim, Kinetics and equilibrium study for the adsorption of textile dyes on coconut shell activated carbon, *Arab. J. Chem.*, 10 (2017) 3381–3396.
- [58] G. Thirupathi, C.P. Krishnamoorthy, S. Pushpavanam, Adsorption characteristics of inorganic salts and detergents on sand beds, *Chem. Eng. J.*, 125 (2007) 177–186.
- [59] N. Singh, Adsorption of herbicides on coal fly ash from aqueous solutions, *J. Hazard. Mater.*, 168 (2009) 233–237.
- [60] J.S. Tarek, T.A. Gad-Allah, H.S. Ibrahim, S.S. Tamer, Adsorption and isothermal models of atrazine by zeolite prepared from Egyptian kaolin, *Solid State Sci.*, 13 (2011) 198–203.
- [61] M.A. Chimdessa, Removal of 2,4-d, Atrazine and Major Metabolites of Atrazine From Aqueous Solution by Fe-Zr-Mn Nanocomposite, Haramaya University, Ethiopia, 2015.
- [62] J. Lemic, D. Kovacevic, M.T. Canovic, D. Kovacevic, T. Stanic, R. Pfend, Removal of atrazine, lindane and diazinone from water by organo-zeolites, *Water Res.*, 40 (2006) 1079–1085.
- [63] J.B. Alam, A.K. Dikshit, M. Bandyopadhyay, Efficacy of adsorbents for 2,4-d and atrazine removal from water environment, *Glob. Nest.*, 2 (2000) 139–148.
- [64] P. Atkins, *Físico-Química*, 6th ed., LTC, Rio de Janeiro, 1997.
- [65] N. Rambabu, C.A. Guzman, J. Soltan, V. Himabindu, Adsorption characteristics of atrazine on granulated activated carbon and carbon nanotubes, *Chem. Eng. Technol.*, 35 (2012) 272–280.
- [66] S.A. Khan, R. Ur-Rehman, M.A. Khan, Adsorption of chromium (III), chromium (VI) and silver (I) on bentonite, *Waste Manag.*, 15 (1995) 271–282.
- [67] Y. Yu, Y.-Y. Zhuang, Z.-H. Wang, Adsorption of water-soluble dye onto functionalized resin, *J. Colloid Interface Sci.*, 242 (2001) 288–293.